Journal Name

ARTICLE

Received 00th January 20xx,
Accepted 00th January 20xx

DOI: 10.1039/x0xx00000x

www.rsc.org/

Lanthanoid Complexes Supported by Retro-Claisen Condensation Products of *β*-Triketonates

Laura Abad Galán,[a,b] Alexandre N. Sobolev,[c] Eli Zysman-Colman,[*b] Mark I. Ogden,[*a] and Massimiliano Massi[*a]

β-Triketonates have been recently used as chelating ligands for lanthanoid ions, presenting unique structures varying from polynuclear assemblies to polymers. In an effort to overcome low solubility of the complexes of tribenzoylmethane, four *β*-triketones with higher lipophilicity were synthesised. Complexation reactions were performed for each of these molecules using different alkaline bases in alcoholic media. X-ray diffraction studies suggested that the ligands were undergoing decomposition under the reaction conditions. This is proposed to be caused by *in situ* retro-Claisen condensation reactions, consistent with two examples that have been reported previously. The lability of the lanthanoid cations in the presence of a varying set of potential ligands gave rise to structures where one, two, or three of the molecules involved in the retro-Claisen condensation reaction were linked to the lanthanoid centres. These results, along with measurements of ligand decomposition in the presence of base alone, suggest that using solvents of lower polarity will mimimise the impact of the retro-Claisen condensation in these complexes.

Introduction

A variety of strategies for the design of luminescence trivalent lanthanoid compounds have been developed in the last few decades, due to their potential use as materials for biological imaging, optical display applications, night vision devices or telecommunication.[1–7] *β*-Triketones are one of the most recent ligand systems found to effectively sensitise the lanthanoid cations, with remarkable photophysical properties for the near-infrared emitters, in particular.[8] Furthermore, lanthanoid *β*-triketonate-based complexes present characteristic structures where discrete tetranuclear assemblies Ae_2Ln_2 can be linked to form polymers $\{Ae_2Ln_2\}_n$ depending on the synthetic conditions.[9,10] The low solubility of these complexes in non-polar solvents drove us to synthesise more lipophilic examples of *β*-triketones, and we report here the syntheses of dm**tbm**H (tris(3,5-dimethylbenzoyl)methane), et**tbm**H (tris(4-ethylbenzoyl)methane), bu**tbm**H (tris(4-butylbenzoyl)methane) and *t*-bu**tbm**H (tris(4-*tert*-butylbenzoyl)methane) (see Figure 1). Given that the crystallised species are dependent on their specific solubility, the modification of the substituents may have an impact on products isolated from the reaction mixture. Hence changes in the synthetic conditions were investigated with the use of different solvents (methanol and ethanol) and different alkali salts (KOH, CsOH).

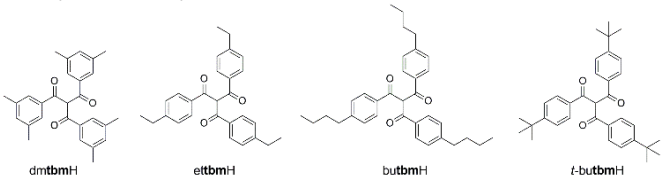

Figure **1**.- Chemical structures of ligands used for this investigation.

In carrying out such work, it is important to note that two cases of a possible *in situ* retro-Claisen condensation reaction were reported for both **tbm**H (tribenzoylmethane)[11] and m**tbm**H (tris(4-methylbenzoyl)methane) molecules,[10] suggesting that the stability of the *β*-triketonates in basic ethanolic solutions during complexation may be an issue. There is some precedent for a similar behaviour with the *β*-diketonates, including an example where retro-Claisen condensation gives rise to a Ti/Sr complex of the diketonate and associated carboxylate[12], but detailed studies of this

[a] School of Life and Molecular Science and Curtin Institute for Functional Molecules and Interfaces, Curtin University, Kent Street, Bentley 6102 WA, Australia.
[b] Organic Semiconductor Centre, EaStCHEM School of Chemistry, University of St. Andrews, St. Andrews, Fife, KY16 9ST, United Kingdom
[c] School of Molecular Sciences, M310, University of Western Australia, Crawley 6009 WA, Australia.
*E-mail: m.massi@curtin.edu.au; m.ogden@curtin.edu.au; eli.zysman-colman@st-andrews.ac.uk
† Electronic Supplementary Information (ESI) available: See DOI: 10.1039/x0xx00000x

phenomenon under conditions relevant for metal complexation do not appear to have been carried out. *In situ* oxidation of dibenzoylmethane has been proposed to explain the presence of phenylglyoxylate in a lanthanum cluster,[13] but the persistence of the diketonate in the triketonate systems mentioned above suggests that a retro-Claisen condensation is the more plausible decomposition pathway.

We report here the isolation of different families of complexes resulting from the reaction of these new *β*-triketones with lanthanoid cations. The results suggest that the impact of the retro-Claisen condensation reaction can be significant under the reaction conditions used. Photophysical studies were conducted in the solid state to elucidate the effect of the composition and structure on the emission properties of the complexes.

Experimental

General procedures

All reagents and solvents were purchased from chemical suppliers and used as received without further purification. Hydrated $LnCl_3$ (Ln = Eu^{3+}, Er^{3+}, Yb^{3+}) was prepared by the reaction of Ln_2O_3 with hydrochloric acid (5 M), followed by evaporation of the solvent under reduced pressure. Infrared spectra (IR) were recorded on solid-state samples using an attenuated total reflectance Perkin Elmer Spectrum 100 FT-IR. IR spectra were recorded from 4000 to 650 cm^{-1}; the intensities of the IR bands are reported as strong (s), medium (m), or weak (w), with broad (br) bands also specified. Melting points were determined using a BI Barnsted Electrothermal 9100 apparatus. Elemental analyses were obtained at Curtin University, Australia. Nuclear magnetic resonance (NMR) spectra were recorded using a Bruker Avance 400 spectrometer (400.1 MHz for ^1H; 100 MHz for ^{13}C) at 300 K. The data were acquired and processed by the Bruker TopSpin 3.1 software. All of the NMR spectra were calibrated to residual solvent signals.

Selected equations.

The values of the radiative lifetime (τ_R), and intrinsic quantum yield (Φ^{Ln}_{Ln}), can be calculated with the following equations.[36]

$$\frac{1}{\tau_R} = 14.65\ s^{-1} \times n^3 \times \frac{I_{Tot}}{I_{MD}} \qquad \text{(Equation 1)}$$

In equation 1, the refractive index (n) of the solvent is used (assumed value of 1.5 in the solid state). The value 14.65 s^{-1} is the spontaneous emission probability of the $^7F_1 \leftarrow {}^5D_0$ transition reported previously. I_{Tot} is the total integration of the Eu^{3+} emission spectrum, and I_{MD} is the integration of the $^7F_1 \leftarrow {}^5D_0$ transition.

$$\Phi^{Ln}_{Ln} = \frac{\tau_{obs}}{\tau_R} \qquad \text{(Equation 2)}$$

The sensitisation efficiency (η_{sens}) can be determined using equation 3 below:

$$\eta_{sens} = \frac{\Phi^{L}_{Ln}}{\Phi^{Ln}_{Ln}} \qquad \text{(Equation 3)}$$

Synthesis

Synthesis of dmdbmH, etdbmH, budbmH and t-budbmH

The dm**dbm**H precursor was synthesised following the same procedure that the previously reported for m**dbm**H[14]. Ethyl 3,5-dimethylbenzoate (3 mmol, 1 eq.) and 1-(3,5-dimethylphenyl)ethanone (3 mmol, 1 eq.) were combined in 40 mL THF. To this solution, a suspension of NaH (60% in mineral oil, 9.0 mmol, 3 eq.) in 40 mL THF was added dropwise at 0 ºC. After one hour, the combined mixture was heated to 40 ºC for 16 hours under nitrogen atmosphere. The solvent was then removed under reduced pressure and water (20 mL) was added to the residual solid paste. The pH was adjusted approximately to neutral by addition of HCl solution (1 M). The aqueous phase was then extracted with ethyl acetate (3 x 15 mL) and the combined organic phase was dried over $MgSO_4$. After filtration, the crude product was obtained by removal of the solvent under reduced pressure and the target compound was isolated, following purification *via* column chromatography in a mixture hexane: ethylacetate (90:10), as a yellow solid.

A similar procedure was followed for the other precursors, substituting in the appropriate ester and ketone with yields 60-80%. The spectroscopic data match those previously reported.[15]

Synthesis of dmtbmH, ettbmH, butbmH and t-butbmH (R-tbmH)

md**tbm**H: 3,5-dimethylbenzoic acid (625 mg, 4.8 mmol) was added to thionyl chloride (5 mL) and heated at reflux for 2 hours. After this time, the solvent was removed under reduced pressure and the remaining solid 3,5-dimethylbenzoyl chloride was immediately added to diethyl ether (20 mL). NaH (60% in mineral oil, 144 mg, 3.6 mmol) and dm**dbm**H (300 mg, 1.2 mmol) were combined in 20 mL diethyl ether and the suspension was maintained at 0 ºC. To this suspension, the solution of 3,5-dimethylbenzoyl chloride in diethyl ether was added dropwise. After the addition, the mixture was stirred under nitrogen atmosphere at 40 ºC for 16 hours. The formed precipitate was filtered and washed with a HCl solution (1 M). The solid was then dried under reduced pressure for several hours, and afforded the target compound as a white solid. Yield 88%. M.p. 194-196 °C. Elemental analysis calcd (%) for $C_{28}H_{28}O_3$: C, 81.52; H, 6.84; found: C, 81.66; H, 6.77. IR (ATR): ν = 2918 w, 2863 w, 1735 s, 1661 s, 1640 s, 1596 m, 1444 m, 1381 m, 1357 w, 1326 m, 1298 s, 1242 m, 1197 w, 1175 s, 1161 s, 1125 m, 1100 s, 1082 m, 1067 m, 1039 m, 1011 w, 995 w, 947 w, 929 m, 895 m, 867 m, 848 m, 812 m, 772 m, 748 m, 713 m. ^1H-NMR (400 MHz, $CDCl_3$) δ 7.54 (dt, J = 1.6, 0.8 Hz,

6H), 7.24 (tt, J = 1.6, 0.8 Hz, 3H), 7.08 (s, 1H), 2.36 (s, 18H).^{13}C-NMR (101 MHz, $CDCl_3$) δ 192.67, 138.61, 135.59, 126.46, 66.14, 21.27.

A similar procedure was followed for the ligands, substituting in the appropriate ester and ketone.

ettbmH: Yield 60%. M.p. 210-212 °C. Elemental analysis calcd (%) for $C_{28}H_{28}O_3$: C, 81.52; H, 6.84; found: C, 81.59; H, 6.84. IR (ATR): ν =3058 w, 2967 w, 1668 s, 1629 m, 1603 s, 1571 m, 1509 w, 1464 m, 1412 m, 1355 m, 1287 s, 1214 m, 1181 s, 1122 m, 1059 w, 1019 w, 1007 m, 961 w, 928 w, 909 w, 863 s, 822 s, 741 m. ^{1}H-NMR (400 MHz, $CDCl_3$) δ 7.86 (d, J = 8.4 Hz, 6H), 7.27 (d, J = 8.6 Hz, 6H), 7.08 (s, 1H), 2.70 (q, J = 7.6 Hz, 6H), 1.24 (t, J = 7.6 Hz, 9H).^{13}C-NMR (101 MHz, $CDCl_3$) δ 191.97, 151.19, 133.71, 129.16, 128.61, 77.16, 66.41, 29.13, 15.20.

butbmH: Yield 55%. M.p. 260-262 °C. Elemental analysis calcd (%) for $C_{34}H_{40}O_3.H_2O$: C, 79.34; H, 8.22; found: C, 79.44; H, 7.89. IR (ATR): ν = 2929 m, 2957 m, 2859 m, 1930 w, 1688 s, 1667 s, 1604 s, 1571 m, 1508 w, 1459 w, 1433 w, 1412 m, 1377 w, 1038 m, 1284 s, 1261 m, 1213 m, 1181 s, 1120 w, 1006 s, 1011 m, 960 w, 931 w, 910 w, 860 s, 832 m, 819 w, 778 w,730 w, 743 w. ^{1}H-NMR (400 MHz, $CDCl_3$) δ 7.85 (d, *J* = 8.3 Hz, 6H), 7.08 (s, 1H), 2.73 – 2.57 (m, 6H), 1.67 – 1.54 (m, 7H), 1.44 – 1.29 (m, 6H), 0.92 (t, *J* = 7.3 Hz, 9H).^{13}C-NMR (101 MHz, $CDCl_3$) δ 191.79, 149.78, 133.55, 128.98, 66.25, 35.72, 33.10, 22.31, 13.87.

***t*-butbm**H: Yield 88%. M.p. 267-269 °C. Elemental analysis calcd (%) for $C_{34}H_{40}O_3$: C, 82.22; H, 8.12; found: C, 81.91; H, 8.15. IR (ATR): ν = 2961 w, 2919w, 2866 w, 1736 m, 1697 m, 1661 m, 1639m, 1600 s, 1473 m, 1406 w, 1380 w, 1357 w, 1298 s, 1242 s, 1188 m, 1176 m, 1161 m, 1125 m, 1102 s, 1067 w, 1008 m, 948 w, 929 w, 909 w, 895 w, 861 s, 847 m, 812 m, 748 m, 713 m. ^{1}H-NMR (400 MHz, $CDCl_3$) δ 7.88 (d, *J* = 8.7 Hz, 1H), 7.47 (d, *J* = 8.7 Hz, 1H), 7.13 (s, 0H), 1.32 (s, 5H).^{13}C-NMR (101 MHz, $CDCl_3$) δ 191.91, 157.92, 133.35, 130.80, 128.92, 126.10, 125.40, 77.16, 66.25, 35.37, 31.14.

General procedure for the synthesis of lanthanoid complexes

AeOH (Ae= K, Cs) (4 eq) was added to a mixture containing md**tbm**H, et**tbm**H, or bu**tbm**H (4 eq) and hydrated $LnCl_3$ (ca. 20 mg) in ethanol or methanol (10 mL). The mixture was heated at reflux for 30 minutes and filtered over a glass frit while still hot. The filtered solution was then left undisturbed at ambient temperature and slow evaporation of the solvent over several days afforded crystals suitable for X-ray diffraction.

*[Eu(dm**ba**)(dm**dbm**)(dm**tbm**)HOEt]$_2$ (**1**):* M.p. 147-149 °C. Elemental analysis calcd (%) for $C_{116}H_{122}Eu_2O_{16}.(1.5H_2O)$: C, 66.25; H, 5.99; found: C, 65.88; H, 5.80. IR (ATR): ν = 2916 w, 1534 s, 1505 s, 1426 m, 1349 s, 1318 s, 1269 m, 1213 m, 1161 w, 1131 w, 1089 w, 1038 w, 959 w, 860 m, 790 s, 765 m.

*[Tb(**μ**-dm**ba**)(dm**dbm**)(dm**tbm**)HOEt]$_2$ (**2**): M.p. 146-148 °C. The elemental analysis was variable probably due to co-precipitation of multiple species. IR (ATR): ν = 2916 w, 1535 s, 1507 s, 1425 m, 1351 s, 1320 s, 1269 m, 1212 m, 1161 w, 1131 m, 1021 w, 946 w, 859 m, 789 s, 765 m.*

[Yb(**μ**-dm**ba**)(dm**dbm**)$_2$HOMe]$_2$ *(**3**):* M.p. 288-290 °C. Elemental analysis calcd (%) for $C_{97}H_{106}O_{15}Yb_2.(3.5H_2O)$: C, 60.78; H, 5.73; found: C, 60.49; H, 5.38. IR (ATR): ν = 2914 w, 1505 s, 1372 s, 1326 m, 1270 m, 1216 m, 998 w, 946 w, 859 w, 788 s, 750 m.

*[Yb(**μ**-dm**dbm**)(dm**dbm**)$_2$]$_2$ (**4**):* M.p. 310-312 °C. Elemental analysis calcd (%) for $C_{114}H_{114}O_{12}Yb_2$: C, 67.71; H, 5.68; found: C, 67.29; H, 5.46. IR (ATR): ν = 2914 w, 1552 s, 1508 s, 1459 s, 1373 s, 1312 m, 1271 m, 1210 m, 1160 m, 1103 w, 997 w, 946 w, 856 m, 783 s, 730w.

*[Eu(dm**dbm**)$_4$(Cs)]$_n$ (**5**):* M.p. 267-269 °C. Elemental analysis calcd (%) for $C_{76}H_{76}CsEuO_8$: C, 65.10; H, 5.46; found: C, 4.77; H, 5.08. IR (ATR): ν = 2912 w, 1551 s, 1503 s, 1459 s, 1402 s, 1362 m, 1317 m, 1211 m, 1157 m, 944 w, 857 w, 781 s.

*[Yb(dm**dbm**)$_4$(K)]$_n$ (**6**):* M.p. 243-245 °C. Elemental analysis calcd (%) for $C_{76}H_{76}KO_8Yb.(H_2O)$: C, 67.74; H, 5.83; found: C, 67.53; H, 5.73. IR (ATR): ν = 2914 w, 1551 m, 1508 s, 1459 m, 1384 m, 1323 m, 1210 m, 1159 m, 1103 w, 996 w, 856 m, 782 s, 730 w.

*[Yb(et**dbm**)$_3$(HOMe)]$_2$ (**7**):* M.p. 249-251 °C. Elemental analysis calcd (%) for $C_{58}H_{61}O_7Yb.(2.5H_2O)$: C, 64.02; H, 6.11; found: C, 63.73; H, 5.84. IR (ATR): ν = 2965 w, 1586 m, 1520 s, 1489 s, 1422 s, 1379 s, 1309 s, 1225 m, 1182 s, 1112 w, 1063 s, 1016 w, 937 w, 849 w, 792 m, 717 w.

*[Yb(et**dbm**)$_4$(Cs·OHMe)]$_n$ (**8**):* M.p. 211-213 °C. The elemental analysis was variable probably due to co-precipitation of multiple species. IR (ATR): ν = 2966 w, 1590 s, 1541 m, 1523 s, 1489 s, 1447 s, 1390m, 1308 m, 1224 m, 1182 m, 1110 m, 11063 m, 1017 m, 941 w, 850 m, 792 m, 715 w.

*[Eu(et**tbm**)$_4$(Cs·HOEt)]$_2$ (**9**):* M.p. 267-269 °C. The elemental analysis was variable probably due to co-precipitation of multiple species. IR (ATR): ν = 2964 w, 1637 w, 1604 w, 1577 m, 1540 s, 1452 w. 1412 m, 1365 s, 1307 m, 1277 m, 1184 w, 1152 m, 1116 w, 1080 w, 1020 w, 964 w, 900 s, 837 m, 796 m, 772 w.

*[Eu(bu**dbm**)$_4$Cs]$_n$ (**10**):* M.p. 214-216 °C. Elemental analysis calcd (%) for $C_{92}H_{108}CsEuO_8$: C, 67.93; H, 6.69; found: C, 67.63; H, 6.75. IR (ATR): ν = 2925 w, 1590s, 1520 s, 1496 s, 1441 s, 1397 m, 1303 m, 1223 m, 1183 m, 1110 w, 1018 w, 939 w, 850 m, 772 s, 710w.

Crystallography

Crystallographic data for the structures were collected at 100(2) K on an Oxford Diffraction Gemini or Xcalibur diffractometer fitted with Mo-Kα or Cu-Kα radiation**.** Data were corrected for Lorentz and polarisation effects and absorption correction. The structures were solved by direct methods and refined by full-matrix least-squares on F^2 using the SHELX-2014 crystallographic package.[49] Unless stated

below, anisotropic displacement parameters were employed for the non-hydrogen atoms. All hydrogen atoms were added at calculated positions and refined by use of a riding model with isotropic displacement parameters based on those of the parent atom. Mercury 3.10.1 was used to visualise, analyse and generate all the graphics included in this investigation.[16] Supplementary crystallographic data can be obtained free of charge *via* http://www.ccdc.cam.ac.uk/conts/retrieving.html, or from the Cambridge Crystallographic Data Centre, 12 Union Road, Cambridge CB2 1EZ, U.K.; fax: (+44) 1223-336-033; or e-mail: deposit@ccdc.cam.ac.uk

X-ray data refinement

*[Eu(μ-dmba)(dm**dbm**)(dm**tbm**)HOEt]$_2$* ***(1)***: $C_{116}H_{122}Eu_2O_{164}(C_2H_6O)$, M = 2260.32, pale yellow prism, 0.16 x 0.11 x0.08 mm^3, monoclinic, space group P21/n (No. 14), a = 15.0498(1), b = 20.7837(1), c = 19.1261(2) Å, β = 110.583(1)°, V = 5600.56(7) Å3, Z = 2, Dc = 1.340 g/cm3, μ = 8.475 mm-1. F000 = 2352, CuKα radiation, λ = 1.54178 Å, T = 100(2)K, 2θmax = 134.6º, 61717 reflections collected, 10001 unique (Rint = 0.0485). Final GooF = 1.000, R1 = 0.0289, wR2 = 0.0667, R indices based on 8766 reflections with I > 2σ (I) (refinement on F2), |Δρ|max= 0.68(6) e Å-3, 697 parameters, 14 restraints. CCDC 1846430

*[Tb(μ-dm**ba**)(dm**dbm**)(dm**tbm**)HOEt]$_2$* ***(2)***: $C_{116}H_{122}Tb_2O_{164}(C_2H_6O)$, M = 2274.25, colorless prism, 0.17 × 0.14 × 0.10 mm^3, monoclinic, space group $P2_1/n$ (No. 14), a = 15.0467(1), b = 20.8306(1), c = 19.1237(2) Å, β = 110.933(1)°, V = 5598.36(7) Å^3, Z = 2, D_c = 1.349 g/cm^3, μ = 6.671 mm^{-1}. F_{000} = 2360, CuKα radiation, λ = 1.54178 Å, T = 100(2)K, $2\theta_{max}$ = 134.6º, 55865 reflections collected, 9972 unique (R_{int} = 0.0311). Final GooF = 1.002, R1 = 0.0241, wR2 = 0.0607, R indices based on 9188 reflections with I > 2σ(I) (refinement on F^2), $|\Delta\rho|_{max}$= 0.46(5) e Å^{-3}, 715 parameters, 8 restraints. CCDC 1846434

*[Yb(μ-dm**ba**)(dm**dbm**)$_2$HOMe]$_2$* ***(3)***: $C_{97}H_{106}O_{15}Yb_2$, M = 1857.90, pale yellow plate, 0.30 × 0.27 × 0.12 mm^3, monoclinic, space group $P2_1/c$ (No. 14), a = 18.0271(3), b = 14.4367(2), c = 34.8079(3) Å, β = 102.091(1)°, V = 8857.9(2) Å^3, Z = 4, D_c = 1.393 g/cm^3, μ = 4.306 mm^{-1}. F_{000} = 3792, CuKα radiation, λ = 1.54178 Å, T = 100(2)K, $2\theta_{max}$ = 135.4º, 26738 reflections collected, 26738 unique (R_{int} = 0.0000). Final GooF = 1.251, R1 = 0.0696, wR2 = 0.1772, R indices based on 25451 reflections with I > 2σ(I) (refinement on F^2), $|\Delta\rho|_{max}$= 2.0(1) e Å^{-3}, 1050 parameters, 7 restraints. CCDC 1846433

*[Yb(μ-*dmdbm*)(dm**dbm**)$_2$]$_2$* ***(4)***: $C_{114}H_{114}O_{12}Yb_2$, M = 2022.13, yellow needle, 0.38 × 0.25 × 0.08 mm^3, monoclinic, space group $P2_1/n$ (No. 14), a = 17.1570(2), b = 14.8841(1), c = 19.6698(2) Å, β = 108.494(1)°, V = 4763.60(8) Å^3, Z = 2, D_c = 1.410 g/cm^3, μ = 2.014 mm^{-1}. F_{000} = 2068, MoKα radiation, λ = 0.71073 Å, T = 100(2)K, $2\theta_{max}$ = 75.3º, 161830 reflections collected, 24607 unique (R_{int} = 0.0543). Final GooF = 1.003, R1 = 0.0391, wR2 = 0.0841, R indices based on 18359 reflections with I > 2σ(I) (refinement on F^2), $|\Delta\rho|_{max}$= 5.0(1) e Å^{-3}, 589 parameters, 0 restraints. CCDC 1846437

*[Eu(dm**dbm**)$_4$(Cs)]$_n$* ***(5)***: $C_{76}H_{76}CsEuO_8$, M = 1402.23, colourless prism, 0.25 × 0.20 × 0.15 mm^3, orthorhombic, space group Pccn (No. 56), a = 14.7842(3), b = 29.7258(5), c = 7.5735(2) Å, V = 3328.34(12) Å^3, Z = 2, D_c = 1.399 g/cm^3, μ = 1.536 mm^{-1}. F_{000} = 1428, MoKα radiation, λ = 0.71073 Å, T = 100(2)K, $2\theta_{max}$ = 64.9º, 65961 reflections collected, 5842 unique (R_{int} = 0.0393). Final GooF = 1.002, R1 = 0.0505, wR2 = 0.1589, R indices based on 4609 reflections with I 2σ(I) (refinement on F^2), $|\Delta\rho|_{max}$= 6.1(2) e Å^{-3}, 222 parameters, 13 restraints. CCDC 1846431

*[Yb(dm**dbm**)$_4$(K)]$_n$* ***(6)***: $C_{76}H_{76}KO_8Yb$, M = 1329.51, colourless needle, 0.07 × 0.03 × 0.02 mm^3, orthorhombic, space group Pccn (No. 56), a = 14.6365(7), b = 29.8941(14), c = 7.4973(7) Å, V = 3280.4(4) Å^3, Z = 2, D_c = 1.346 g/cm^3, μ = 3.641 mm^{-1}. F_{000} = 1370, CuKα radiation, λ = 1.54178 Å, T = 100(2)K, $2\theta_{max}$ = 134.6º, 22647 reflections collected, 2928 unique (R_{int} = 0.1196). Final GooF = 1.009, R1 = 0.0851, wR2 = 0.2296, R indices based on 1781 reflections with I > 2σ(I) (refinement on F^2), $|\Delta\rho|_{max}$= 3.8(2) e Å^{-3}, 222 parameters, 13 restraints. CCDC 1846432

*[Yb(et**dbm**)$_3$(HOMe)]$_2$* ***(7)***: $C_{58}H_{61}O_7Yb$, M = 1043.10, yellow needle, 0.31 × 0.23 × 0.17 mm^3, monoclinic, space group $P2_1/c$ (No. 14), a = 27.6844(3), b = 12.2823(1), c = 30.1388(3) Å, β = 105.316(1)°, V = 9884.06(17) Å^3, Z = 8, D_c = 1.402 g/cm^3, μ = 1.945 mm^{-1}. F_{000} = 4280, MoKα radiation, λ = 0.71073 Å, T = 100(2)K, $2\theta_{max}$ = 64.9º, 204134 reflections collected, 33939 unique (R_{int} = 0.0415). Final GooF = 1.002, R1 = 0.0449, wR2 = 0.1146, R indices based on 28533 reflections with I > 2σ(I) (refinement on F^2), $|\Delta\rho|_{max}$= 3.9(1) e Å^{-3}, 1206 parameters, 13 restraints. CCDC 1846438

*[Yb(et**dbm**)$_4$(Cs·OHMe)]$_n$* ***(8)***: $C_{78}H_{84}CsO_{10}Yb$, M = 1487.40, colourless needle, 0.24 × 0.19 × 0.08 mm^3, monoclinic, space group C2 (No. 5), a = 30.1708(10), b = 8.3962(1), c = 14.9290(9) Å, β = 118.445(4)°, V = 3325.3(2) Å^3, Z = 2, D_c = 1.486 g/cm^3, μ = 2.006 mm^{-1}. F_{000} = 1442, MoKα radiation, λ = 0.71073 Å, T = 100(2)K, $2\theta_{max}$ = 65.4º, 18749 reflections collected, 18749 unique (R_{int} = 0.0000). Final GooF = 1.000, R1 = 0.0368, wR2 = 0.1007, R indices based on 17754 reflections with I > 2σ(I) (refinement on F^2), $|\Delta\rho|_{max}$= 5.5(1) e Å^{-3}, 414 parameters, 1 restraint. Absolute structure parameter = 0.010(5)[17] The structure refined as a 2-component twin. Component 2 rotated by -179.9953° around [1.00 0.00 0.01] (reciprocal) or [0.71 0.00 0.71] (direct) direction. CCDC 1846429

*[Eu(et**tbm**)$_4$(Cs·HOEt)]$_2$* ***(9)***: $C_{228}H_{228}Cs_2Eu_2O_{26}$, M = 3953.84, colourless needle, 0.25 × 0.09 × 0.06 mm^3, triclinic, space group P-1 (No. 2), a = 17.1680(5), b = 17.4332(4), c = 18.4379(3) Å, α = 88.513(2), β = 80.968(2), γ = 65.713(2)°, V = 4963.0(2) Å^3, Z = 1, D_c = 1.323 g/cm^3, μ = 7.829 mm^{-1}. F_{000} = 2040, CuKα radiation, λ = 1.54178 Å, T = 100(2)K, $2\theta_{max}$ = 134.6º, 109457 reflections collected, 17676 unique (R_{int} = 0.0557). Final GooF = 1.034, R1 = 0.0707, wR2 = 0.1979, R

indices based on 14055 reflections with I > 2σ(I) (refinement on F²), $|\Delta\rho|_{max}$= 1.57(9) e Å^{-3}, 1049 parameters, 732 restraints. CCDC 1846436

*[Eu(bu**dbm**)$_4$Cs]$_n$* ***(10)**:* $C_{92}H_{108}CsEuO_8$, M = 1626.65, colourless plate, 0.38 × 0.25 × 0.18 mm³, monoclinic, space group I2 (No. 5), a = 21.3014(2), b = 8.0066(1), c = 23.7700(3) Å, β = 99.984(1)°, V = 3992.62(8) Å³, Z = 2, D_c = 1.353 g/cm³, μ = 1.291 mm^{-1}. F_{000} = 1684, MoKα radiation, λ = 0.71073 Å, T = 100(2)K, $2\theta_{max}$ = 64.1º, 42702 reflections collected, 13119 unique (R_{int} = 0.0238). Final GooF = 1.004, R1 = 0.0277, wR2 = 0.0688, R indices based on 12624 reflections with I > 2σ(I) (refinement on F²), $|\Delta\rho|_{max}$= 1.89(8) e Å^{-3}, 465 parameters, 1 restraint. Absolute structure parameter = 0.014(7)[17] CCDC 1846428

*t-bu**tbm**H:* $C_{34}H_{40}O_3$, M = 496.66, colourless needle, 0.28 × 0.08 × 0.03 mm³, monoclinic, space group P21/n (No. 14), a = 12.7501(3), b = 10.0565(2), c = 22.7503(5) Å, β = 97.672(2)°, V = 2890.96(11) Å³, Z = 4, D_c = 1.141 g/cm³, μ = 0.553 mm^{-1}. F_{000} = 1072, CuKα radiation, λ = 1.54178 Å, T = 100(2)K, $2\theta_{max}$ = 134.6º, 25300 reflections collected, 5149 unique (R_{int} = 0.0570). Final GooF = 1.002, R1 = 0.0438, wR2 = 0.1048, R indices based on 3870 reflections with I > 2σ(I) (refinement on F²), $|\Delta\rho|_{max}$= 0.21(4) e Å^{-3}, 343 parameters, 0 restraints. CCDC 1846435

Results and discussion

Synthesis of the lanthanoid assemblies. The dm**tbm**H, et**tbm**H, bu**tbm**H and *t*-bu**tbm**H molecules were synthesised following the procedure previously reported for **tbm** and m**tbm**.[8,10] When the ligands were made to react with hydrated $LnCl_3$ (Ln^{3+} = Eu, Tb, Yb) in the presence of AeOH (Ae^+ = K, Cs) in ethanol or methanol, species containing products of the retro-Claisen condensation reaction of the triketonate molecules were found. The isolated complexes were identified by X-ray diffraction and confirmed by means of IR spectroscopy and elemental analysis when possible as co-precipitation of multiple species was observed in various cases (see Experimental).

The two retro-Claisen condensation products of the *β*-triketone are the associated *β*-diketonate and benzoate anions.[18] Consequently, three potential ligands can be present in the complexation mixture: *β*-triketonates, *β*-diketonates and benzoates.

In the case of dm**tbm**H, the isolated complexes can be classified in three distinct families depending on the number of different species directly coordinated to the lanthanoid centre (see Figure 2):

a) Three species: [Ln(*μ*-dm**ba**)(dm**dbm**)(dm**tbm**)(HOEt)]$_2$, where Ln^{3+}= Eu (**1**), Tb (**2**)
b) Two species: [Yb(*μ*-dm**ba**)(dm**dbm**)$_2$(HOMe)]$_2$ (**3**)
c) One specie: [Yb(μ-dm**dbm**)(dm**dbm**)$_2$]$_2$ (**4**), [Ln(dm**dbm**)$_4$(Ae)]$_n$ where Ln^{3+} = Eu, Yb, Ae^+= Cs, K (**5**, **6**).

A similar behaviour was found for the et**tbm**H molecule with the isolated complexes confirming retro-Claisen condensation reactivity; [Yb(et**dbm**)$_3$(HOMe)] (**7**), [Yb(et**dbm**)$_4$(Cs)]$_n$ (**8**). Furthermore, one structure was identified to contain only the unreacted *β*-triketonate ligand, [Eu(et**tbm**)$_4$(Cs·HOEt)]$_2$ (**9**), following the formula previously reported for the tetranuclear assemblies (see Figure **3**).[9]

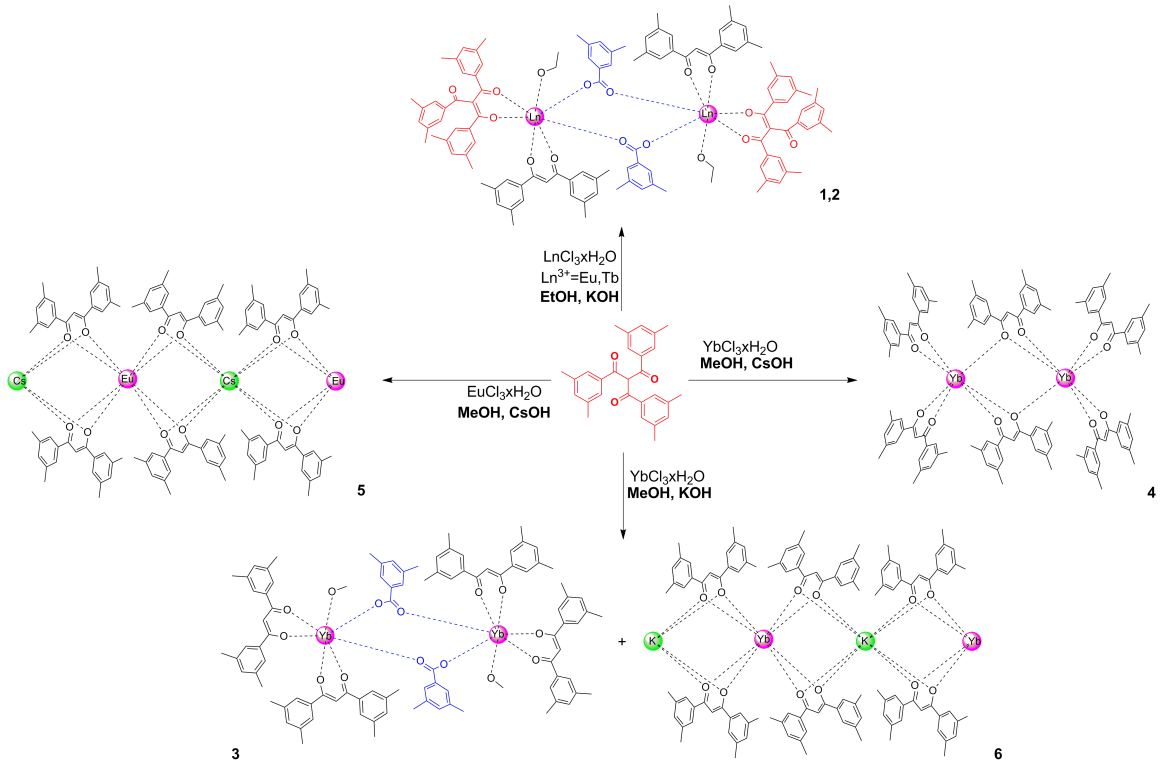

Figure **2.** Summary of the isolated assemblies according to reaction conditions for the **dmtbm**H molecule.

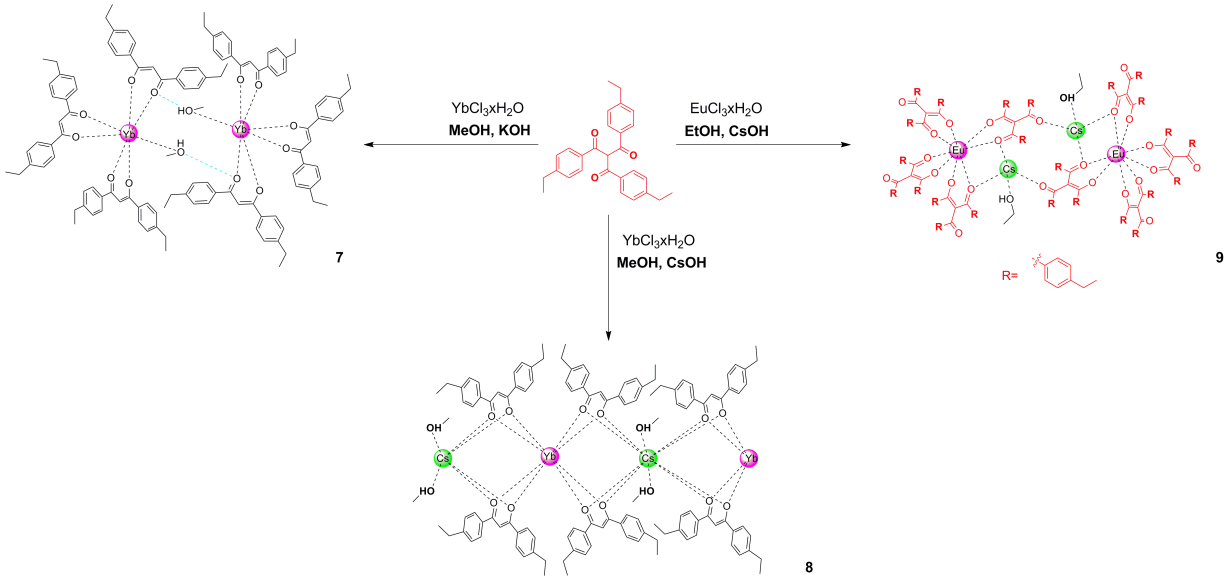

Figure **3**. Summary of the isolated assemblies according to reaction conditions for the et**tbm**H molecule.

Finally, when analogous complexation reactions were followed for the bu**tbm**H and *t*-bu**tbm**H molecules, only one crystalline material was isolated (see Figure **4**), $[Eu(bu\mathbf{dbm})_4(Cs)]_n$ (**10**). Less polar solvents were also tested for these ligands. Unfortunately, when one equivalent of $Ln(NO_3)_3{\cdot}DMSO_n$ (Ln^{3+}= Eu^{3+}, Yb^{3+}) was reacted with four equivalents of the *t*-bu**tbm**H in the presence of four equivalents of potassium *tert*-butoxide in acetonitrile, only the *t*-bu**tbm**H molecule crystallised (see SI).

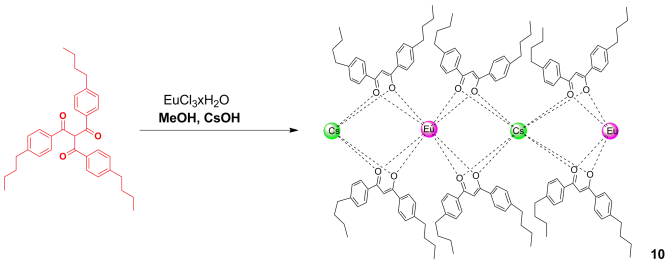

Figure **4**. Summary of the isolated assemblies according to reaction conditions for the bu**tbm**H molecule.

NMR studies.

To further elucidate the stability of the *β*-triketonate molecules in basic alcoholic conditions, ^{1}H-NMR studies were first performed in the absence of the lanthanoid cations. The different solutions, prepared in d_4-methanol by addition of the correspondent *β*-triketonate and 1 equivalent of KOH (10^{-2} M), were monitored by ^{1}H-NMR every 24 hours. In every case, mixtures of *β*-triketonates and *β*-diketonates, in both tautomeric forms, and their corresponding benzoates could be detected in solution over time, resulting in convoluted spectra. The ratio between the integration of the aromatic proton, for the β-triketonate, and the constant integration of the solvent peak, was plotted against time to quantify the progression of the retro-Claisen condensation in these systems. High decomposition rates were noted for all triketone molecules, with almost 80% lost in the case of et**tbm**H after 5 days (Figure 5). The most stable β-triketonate is **tbm** with 30% lost after 5 days, which may explain why retro-Claisen condensation of this molecule was not observed in earlier work on the triketonates.[9,19] Finally, these results show that bu**tbm**H and *t*-bu**tbm**H undergo the retro-Claisen condensation to similar extents. Therefore, the fact that examples of complexes based on these ligands have yet to be isolated may be related difficulties in crystallising the resulting complexes rather than their initial formation.

As the least stable of the triketonates examined, et**tbm**H was then tested in d_6-ethanol solution under similar conditions. In this case, it was found that the stability is significantly enhanced with only 2% of et**tbm** lost over the same time and therefore there is negligible appearance of the retro-Claisen condensation products after 5 days. These results are in agreement with the experimentally isolated structures from ethanol, which all included unreacted *β*-triketonate either exclusively, or as part of a ligand mixture.
Finally, similar studies were performed in the presence of base and the lanthanoid cations. Retro-Claisen condensation seemed to be significantly more rapid in the presence of the *f* elements, which results in highly convoluted spectra that were not further analysed (see SI).

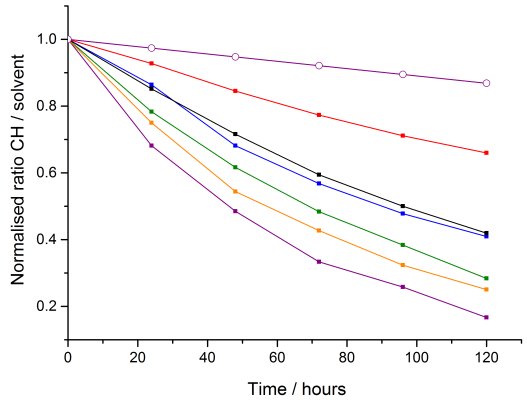

Figure **5**. Ratio of retro-Claisen condensation reactivity over the time for the **tbm** (red trace), m**tbm** (blue trace), dm**tbm** (black trace), et**tbm** (purple trace), bu**tbm** (green trace), *t*-bu**tbm** (orange trace) molecules all in *d*-MeOH (squares) and *d*-EtOH (circles).

Crystal structures

*a) Products of the reaction of dm**tbm**H with lanthanoids, Ln=Eu^{3+},Tb^{3+}, Yb^{3+}*

The structures for the [Ln(*μ*-dm**ba**)(dm**dbm**)(dm**tbm**)(HOEt)]$_2$ Ln^{3+}= Eu (**1**), Tb (**2**) are isomorphous and can be described as a dimer formed by two Ln^{3+}, two *β*-triketonates, two *β*-diketonates and two bridging benzoates. Each metal centre is seven coordinated, with one *β*-triketonate and one *β*-diketonate in a bidentate mode, two monodentate benzoate ligands bridging the lanthanoid centres and one molecule of ethanol completing the coordination sphere (**Error! Reference source not found.**). The two Ln^{3+} cations are equivalent, being related by an inversion centre and separated by distances of Eu, 4.051 Å, and Tb, 4.021 Å. Each structure is best described as a capped octahedron (see SI).

A similar structure was found in the case of [Yb(*μ*-dm**ba**)(dm**dbm**)$_2$(HOMe)]$_2$ (**3**) where the dimer is formed by two seven coordinated Yb^{3+} and four *β*-diketonates, rather than two *β*-triketonates and two *β*-diketonates (**Error! Reference source not found.**6). Two benzoate ligands bridge the two Yb^{3+} centres and the coordination sphere is completed by a coordinating molecule of methanol. In this case, the coordination sphere of the two Yb^{3+} cations is slightly different with differing degrees of distortion from a capped octahedron geometry (see SI).

A different dinuclear complex was found for the [Yb(*μ*-dm**dbm**)(dm**dbm**)$_2$]$_2$ (**4**) where only the *β*-diketonate ligand is present in the structure (Figure 6). This arrangement is analogous to the previously published structure formed by Gd^{3+} and 2,2,6,6-tetramethylheptane-3,5-dione.[20] In this case, each Yb^{3+} is seven coordinated, where the main ligand bridges the two lanthanoid centres with no molecules of solvent directly coordinated. The Yb^{3+}···Yb^{3+} distance is slightly shorter in this structure, 3.691 Å, in comparison to the mixed ligand dimers. The structure is best described as a distorted capped trigonal prism.

Because lanthanoid-lanthanoid distances in complexes **1**-**4** are quite short, lanthanoid-lanthanoid cross relaxation quenching should be considered, when studying photophysical properties.[21–23]

Finally, complexes **5**, [Eu(dm**dbm**)$_4$(Cs)]$_n$ and **6**, ([Yb(dm**dbm**)$_4$(K)]$_n$ were identified as linear coordination polymers, following a similar formula to the previously reported structures with dibenzoylmethane (see SI).[24]

*b) Products of the reaction of et**tbm**H with lanthanoids, Ln=Eu^{3+}, Yb^{3+}*

Complex **7** crystallises as a hydrogen bonded dimer involving only the *β*-diketonate ligand and solvent molecules, formulated as [Yb(et**dbm**)$_3$(HOMe)], where each Yb^{3+} is seven coordinated with three *β*-diketonates binding in a bidentate mode and an oxygen atom from a molecule of solvent methanol (Figure 7). The dimer is situated about an inversion centre and is linked by hydrogen bonds between the methanol O atom and keto-O (O22). The resulting pair of lanthanoid ions are relatively close in distance, 5.704 Å, which could cause quenching by energy transfer between lanthanoid excited states. The coordination geometry is best described as a distorted capped trigonal prism.

Complexes **8** ([Yb(et**dbm**)$_4$(Cs·OHMe)]$_n$) and **9**

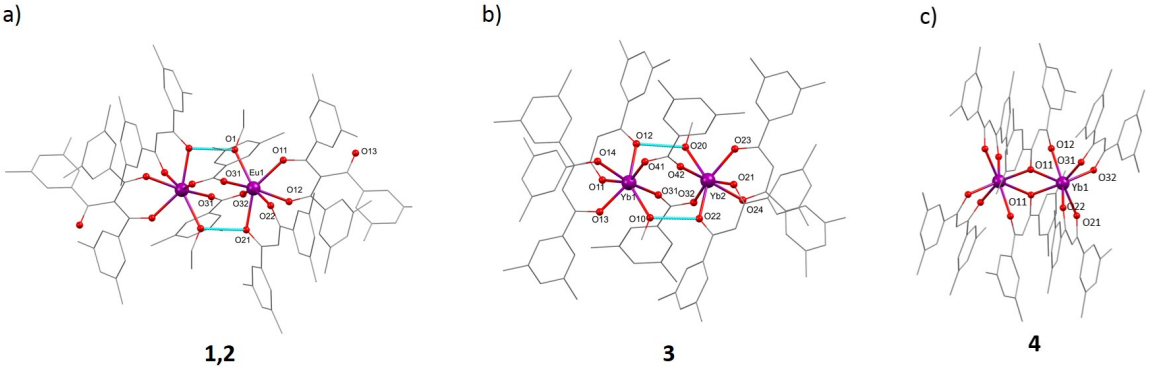

Figure **6**. Representation of the X-Ray crystal structure of a) [Eu(μ-dm**ba**)(dm**dbm**)(dm**tbm**)(HOEt)]$_2$, b) [Yb(μ-dm**ba**)(dm**dbm**)$_2$(HOMe)]$_2$ and c) [Yb(μ-dm**dbm**)(dm**dbm**)$_2$]$_2$ where hydrogens bonds are highlighted in blue. Hydrogens have been omitted for clarity.

([Eu(et**tbm**)$_4$(Cs·OHEt)]$_2$) are analogous to the previously described linear diketonate polymers (**5**, **6**)[24] and reported triketonate-supported tetranuclear assemblies[19], respectively (see SI).

*c) Products of the reaction of bu**tbm**H with lanthanoids, Ln=Eu^{3+}*

The structure of the [Eu(bu**dbm**)$_4$(Cs)]$_n$ (**10**) presents a similar linear polymeric structure to that already described for the dm**tbm**H and et**tbm**H complexes (see SI).

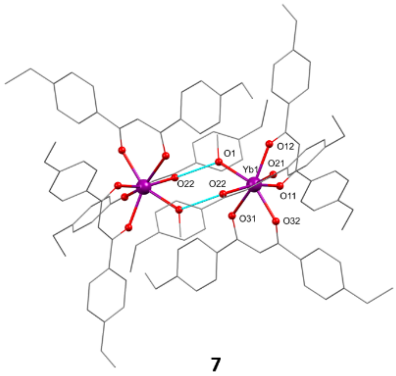

7

Figure **7**. Representation of the X-ray crystal structure of [Yb(et**dbm**)$_3$(HOMe)]$_2$. Hydrogen atoms are omitted for clarity.

Photophysical investigation

The energy of the triplet state of the *β*-triketonates and their corresponding *β*-diketonates were measured at the 0-phonon transition of the phosphorescent emission at 77 K of their corresponding Gd^{3+} complexes. These energies were found to lie close in energy in the region 20,202- 20,844 cm^{-1}, independently of the relative substituent (see SI), as expected. Therefore, these ligands would be expected to effectively sensitise Eu^{3+} ($^5D_0$ = ~17,200 cm^{-1}) and Yb^{3+} ($^2F_{5/2}$ = ~10,200 cm^{-1}) excited states.

The emission properties for complexes where the bulk of the sample was confirmed to be pure by elemental analysis (**1, 3**, **4**, **5**, **6**, **7** and **10)** were recorded in the solid state. In every case, the emission was seen as a consequence of the antenna effect, evidenced by the broad excitation spectra similar to the absorption spectra of the ligands (see SI). The photophysical data, including excited state lifetime decay (τ_{obs}), calculated radiative decay (τ_R), intrinsic photoluminescence quantum yield (Φ_{Ln}^{Ln}) and overall quantum yield (Φ_{Ln}^{L}) are reported in Tables **1** and **2**.

a) Visible light emitters

The emission spectrum of complex **1**, shows the characteristic peaks of Eu^{3+}, attributed to the $^7F_J \leftarrow {}^5D_0$ (J = 0-6) in the region 550-750 nm (Figure 8). [25] The presence of the narrow $^7F_0 \leftarrow {}^5D_0$ peak at 580 nm (full width at half maximum ~40 cm^{-1}) is an indication of a unique low symmetric Eu^{3+} centre. This is in agreement with the crystal structure where the two Eu^{3+} cations present in the dimer are related by an inversion centre. The splitting of the magnetic dipole ($^7F_1 \leftarrow {}^5D_0$) and the hypersensitive transition ($^7F_2 \leftarrow {}^5D_0$) into two and three bands, respectively, is suggestive of trigonal fields. This result is supported by shape analysis where the geometry is best described as capped octahedron (trigonal, C_{3v}). (See SI). The excited state lifetime decay was satisfactorily fitted with a monoexponential function and was measured to be 47 µs (see SI), shorter than analogous *β*-diketonates complexes, suggesting efficient non-radiative decay pathways. These quenching processes may include, multiphonon relaxation due to the EtO-H coordinated to the Eu^{3+} centre, and energy transfer between the two lanthanoid centres separated by a short distance (~4 Å). From the Eu^{3+} spectrum, the value of radiative lifetime can be calculated to be 0.78 ms, giving an intrinsic quantum yield value of 6%. The overall quantum yield was measured using an integrating sphere and was found to be 2%, which implies a poor sensitisation efficiency of 33%. In fact, some direct excitation can be observed in the excitation plot for emission recorded at 612 nm (see SI).

Complexes **5** and **10** show characteristic Eu^{3+} emission in the region 580-750 nm (Figure 8). The $^7F_0 \leftarrow {}^5D_0$ transition is absent in both cases, suggesting that the Eu^{3+} ion occupies a site with higher symmetry than complex **1**. The splitting of the magnetic dipole transition, $^7F_1 \leftarrow {}^5D_0$, and the hypersensitive band, $^7F_2 \leftarrow {}^5D_0$, is slightly different which indicates different degrees of distortion between the two coordination spheres. These trends are confirmed by the results found in the shape analysis (see SI). The excited state lifetimes decay values (τ_{obs}) were measured to be much longer than complex **1** with values of 815 and 485 µs, respectively. These data suggest that lanthanoid cross relaxation quenching is not effective in the linear polymers (**5**, **10**) where the Eu···Eu distance is longer than 8 Å.

The intrinsic quantum yields ($\mathbf{\Phi_{Ln}^{Ln}}$) were found to be 68% and 50%, respectively, based on the radiative lifetimes calculated from the emission spectra. Overall quantum yields were measured to be 45 and 43%, respectively. The photophysical data for the two complexes are therefore comparable, showing high sensitisation efficiency in both cases.

Table 1. Photophysical data for the Eu^{3+} complexes in the solid state

Complex	τ_{obs}(μs)	τ_R(ms)	Φ_{Ln}^{Ln}(%)	Φ_{Ln}^{L} (%)
1	47	0.79	6	2
5	815	1.19	68	45
10	485	0.96	50	43

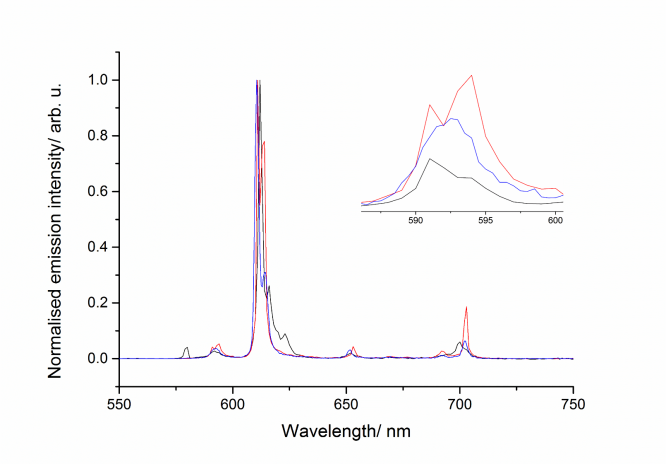

Figure **8**. Normalised emission plots for **1** (black trace), **5** (red trace) and **10** (blue trace) Eu^{3+} complexes, with excitation wavelength at 350 nm. Inset: highlight of the peaks corresponding to the $^7F_1 \leftarrow {}^5D_0$ transition.

b) NIR light emitters

Characteristic Yb^{3+} NIR emission for complexes **3**, **4**, **6** and **7** was observed in the 900-1100 nm region corresponding to the $^2F_{7/2} \leftarrow {}^2F_{5/2}$ transition (Figure 9). Different splitting of this transition is found in the case of the 7-coordinated Yb^{3+} dimers (**3**, **4** and **7**) suggestive of different coordination environments of the lanthanoid centres, which is in agreement with the shape analysis studies (see SI). In contrast, this transition is split into five main bands in the case of the 8-coordinated Yb^{3+} polymer (**6**). In every case, emission from hot bands is present as a shoulder in the 930-960 nm region.[26]

The observed lifetime decays (τ_{obs}) for all the Yb^{3+} complexes were satisfactorily fitted to monoexponential functions. The lifetimes decay values for the Yb^{3+} dimers **3, 4** and **7**, are 10.4, 12.7, 8.0 μs, respectively. These values are comparable to similar reported *β*-diketonate complexes.[27,28] This suggests that the presence of a molecule of methanol coordinated to the lanthanoid cations in complexes **3** and **7** is not dramatically quenching the NIR emission which might be explained by the presence of intramolecular hydrogen bonds with short O…O distances involving the methanol OH groups in both structures (**3**: O10…O22, 2.70(1); O20…O12, 2.74(1). **7**: O1…O22, 2.576(3); O2…O51, 2.578(3) Å). Nevertheless, the lifetime decay for the Yb^{3+} polymer (**6**), which has no coordinated MeOH molecules, was found to be slightly longer with a value of 14.0 μs. However, other quenching effects such as self-quenching could also be occurring, since the Yb^{3+} cations sit relatively close in distance (~4 Å) for complexes **3, 4** and **7**.

Table **2** Photophysical data for the Yb^{3+} complexes in the solid state

Complex	τ_{obs} (μs)	τ_R (ms)[a]	Φ_{Ln}^{Ln}(%)
3	10.4	1.2	0.86
4	12.7	1.2	1.1
6	14.0	1.2	1.2
7	8.0	1.2	0.7

[a] Literature τ_R for Yb^{3+}.[26]

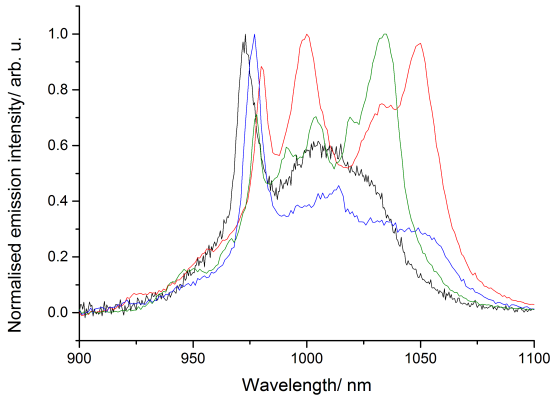

Figure **9.**- Normalised emission plots for **3** (black trace), **4** (red trace), **6** (blue trace) and **7** (green trace) Yb^{3+} complexes, with excitation wavelength at 350 nm.

Conclusions

In this report four new *β*-triketones were synthesised and fully characterised, with the aim of using these as ligands to form lipophilic lanthanoid complexes. It was found that the lanthanoid complexation reaction under basic conditions in polar solvents, methanol or ethanol, yielded structures where their retro-Claisen condensation products were incorporated. The high lability of the lanthanoid cations in the presence of a dynamically changing ligand set gave rise to complexes where one, two or even the three retro-Claisen condensation reactants and products were linked to the lanthanoid centres. These results showed that ligand stability is a significant issue under the complexation reaction conditions that were used. Indeed, when the stability of the *β*-triketones in methanol was studied in basic conditions in the absence of lanthanoid cations, significant decomposition was found in all cases, with a maximum of 80% for the et**tbm**H molecule. Finally, photophysical studies revealed that the majority of the resulted mixed ligand complexes were emissive in the visible or NIR range.

Conflicts of interest

There are no conflicts to declare.

Acknowledgements

This research was partially supported by the Australian Research Council's Discovery *Projects* funding scheme (project DP17010189), and a Royal Society International Exchanges Grant. EZ-C thanks EPSRC (EP/M02105X/1) for support. L.A.G thanks Curtin University for the postgraduate scholarship.

Notes and references

1 A. de Bettencourt-Dias, *Dalton Trans.*, 2007, **22**, 2229–2241.
2 S. V. Eliseeva and J.-C. G. Bünzli, *New J. Chem.*, 2011, **35**, 1165.
3 J.-C. G. Bünzli, *Eur. J. Inorg. Chem.*, 2017, **2017**, 5058–5063.
4 S. V. Eliseeva and J.-C. G. Bünzli, *Chem. Soc. Rev.*, 2010, **39**, 189–227.
5 J. Kido and Y. Okamoto, *Chem. Rev.*, 2002, **102**, 2357–2368.
6 J.-C. G. Bünzli, *Luminescence Bioimaging with Lanthanide Complexes*, 2014, vol. 1st.
7 J.-C. G. Bünzli and S. V. Eliseeva, *J. Rare Earths*, 2010, **28**, 824–842.
8 B. L. Reid, S. Stagni, J. M. Malicka, M. Cocchi, G. S. Hanan, M. I. Ogden and M. Massi, *Chem. Commun.*, 2014, **50**, 11580–11582.
9 B. L. Reid, S. Stagni, J. M. Malicka, M. Cocchi, A. N. Sobolev, B. W. Skelton, E. G. Moore, G. S. Hanan, M. I. Ogden and M. Massi, *Chem. - Eur. J.*, 2015, **21**, 18354–18363.
10 L. Abad Galán, B. L. Reid, S. Stagni, A. N. Sobolev, B. W. Skelton, M. Cocchi, J. M. Malicka, E. Zysman-colman, E. G. Moore, M. I. Ogden and M. Massi, *Inorg. Chem.*, 2017, **56**, 8975–8985.
11 L. Abad Galán, A. N. Sobolev, B. W. Skelton, E. Zysman-colman, I. Mark and M. Massi, *ChemRxiv.*, 2018, 10.26434/chemrxiv.6008294.v1.
12 C. Pettinari, F. Marchetti, R. Pettinari, V. Vertlib, A. Drozdov, I. Timokhin, S. Troyanov, Y. S. Min and D. Kim, *Inorg. Chim. Acta*, 2003, **355**, 157–167.
13 P. C. Andrews, T. Beck, C. M. Forsyth, B. H. Fraser, P. C. Junk, M. Massi and P. W. Roesky, *Dalton Trans.*, 2007, **9226**, 5653–5736.
14 J. Ishida, H. Ohtsu, Y. Tachibana, Y. Nakanishi, K. F. Bastow, M. Nagai, H. K. Wang, H. Itokawa and K. H. Lee, *Bioorganic Med. Chem.*, 2002, **10**, 3481–3487.
15 J. Zawadiak and M. Mrzyczek, *Spectrochim. Acta - Part A Mol. Biomol. Spectrosc.*, 2012, **96**, 815–819.
16 C. F. Macrae, I. J. Bruno, J. A. Chisholm, P. R. Edgington, P. McCabe, E. Pidcock, L. Rodriguez-Monge, R. Taylor, J. Van De Streek and P. A. Wood, *J. Appl. Crystallogr.*, 2008, **41**, 466–470.
17 H. D. Flack, *Acta Crystallogr. Sect. A*, 1983, **39**, 876–881.
18 F. Xie, F. Yan, M. Chen and M. Zhang, *RSC Adv.*, 2014, **4**, 29502–29508.
19 B. L. Reid, S. Stagni, J. M. Malicka, M. Cocchi, G. S. Hanan, M. I. Ogden and M. Massi, *Chem. Commun.*, 2014, **50**, 11580–11582.
20 I. Baxter, S. R. Drake, M. B. Hursthouse, K. M. Abdul Malik, J. McAleese, D. J. Otway and J. C. Plakatouras, *Inorg. Chem.*, 1995, **34**, 1384–1394.
21 C. Piguet, A. F. Williams, J. C. G. Bünzli, G. Bernardinelli and G. Hopfgartner, *J. Am. Chem. Soc.*, 1993, **115**, 8197–8206.
22 A. Nonat, M. Regueiro-Figueroa, D. Esteban-Gõmez, A. De Blas, T. Rodríguez-Blas, C. Platas-Iglesias and L. J. Charbonnière, *Chem. - Eur. J.*, 2012, **18**, 8163–8173.
23 A. Zam, S. V Eliseeva, L. Guønøe, H. Nozary, S. Petoud and C. Piguet, *Chem. - Eur. J.*, 2014, **20**, 12172–12182.
24 D. T. Thielemann, M. Klinger, T. J. a Wolf, Y. Lan, W. Wernsdorfer, M. Busse, P. W. Roesky, A. N. Unterreiner, A. K. Powell, P. C. Junk and G. B. Deacon, *Inorg. Chem.*, 2011, **50**, 11990–12000.
25 K. Binnemans, *Coord. Chem. Rev.*, 2015, **295**, 1–45.
26 J. C. G. Bünzli and S. V. Eliseeva, *Photophysics of Lanthanoid Coordination Compounds*, 2013, vol. 8.
27 S. Dang, J. B. Yu, X. F. Wang, Z. Y. Guo, L. N. Sun, R. P. Deng, J. Feng, W. Q. Fan and H. J. Zhang, *J. Photochem. Photobiol. A Chem.*, 2010, **214**, 152–160.
28 O. Sun, P. Chen, H.-F. Li, T. Gao, W.-B. Sun, G.-M. Li and P.-F. Yan, *CrystEngComm*, 2016, **18**, 4627–4635.

